Evaluation and modelling of a CO selective oxidation reactor for solid polymer fuel cell automotive applications

C.D. Dudfield [*], R. Chen, P.L. Adcock

Department of Aeronautical and Automotive Engineering, Loughborough University, Leicestershire, LE11 3TU, UK

Abstract

On-board methanol reforming is an attractive alternative to direct hydrogen storage for solid polymer fuel cell (SPFC) powered vehicles, due to the increased volumetric energy storage density of methanol. Unfortunately, carbon monoxide is always produced during the reforming reaction. CO rapidly de-activates the platinum electro-catalyst in the fuel cell and must be reduced to levels typically less than 20 ppm. In this paper, the development of a precious metal based catalytic CO oxidation reactor developed by the Fuel Cell Research Group at Loughborough University is reported. A simplified simulation model has also been developed, based upon measured catalyst activity and CO oxidation selectivity. Experimental results from reactor studies show that CO concentrations can be reduced from a typical steam reformer output of 7000 ppm input to ≤ 15 ppm in the presence of approximately 75% hydrogen. Experimental results have shown good agreement with the simulation model. © 2000 Elsevier Science S.A. All rights reserved.

Keywords: Solid polymer fuel cell; CO oxidation reactor; Methanol

1. Introduction

Solid polymer fuel cells (SPFC) are becoming an increasingly attractive technology for electrical power generation since they offer the advantages of high efficiency, zero or virtually zero emissions (depending upon the fuel feedstock) and mechanical robustness. Although technologically elegant, electrical power generation from the cells is simply achieved through the controlled electrochemical combination of hydrogen and oxygen with water being the only reaction product. SPFC systems are suitable for a wide range of applications, and in particular are seen as a realistic and clean alternative to the internal combustion engine [1–5].

Hydrogen is the ideal fuel for the SPFC since it simplifies system integration, maximises system efficiency, provides zero emissions, and allows the best load-following characteristics. There are however, several principle concerns regarding the use of hydrogen in automobiles. In addition to potential safety concerns there is a need for an acceptable refuelling infrastructure. The development of a hydrogen infrastructure should meet both the requirements of customer acceptance and commercial viability. Costs include capitalisation of the fuelling station (e.g. fuel reformer and compressor), the vehicle storage tanks and fuel production itself. Apart from safety and infrastructure concerns, the direct storage of hydrogen on-board a vehicle is also somewhat compromised by its inherent low volumetric energy storage density.

The reforming of hydrocarbons and alcohols is becoming an attractive possibility for SPFC applications due to the ''chemical'' storage of hydrogen at increased energy densities. Methanol, in particular, is receiving considerable attention as the initial fuel of choice due to its low production cost and ease of reformation [3,6–8]. The reforming of various petroleum distillates is also an attractive proposition due to their high energy densities and ease of supply [9,10]. However, difficulties are currently envisaged in reforming efficiently at temperatures suitable for SPFC automotive use, and also in avoiding catalyst poisoning due to the high impurity concentration of such distillates. Technology for converting methanol into a hydrogen rich supply for the fuel cells is currently based upon steam reformation, partial oxidation, or a combination of both (autothermal reforming). Steam reforming offers the advantages of the highest hydrogen yield (up to 75% in theory) and system efficiency at relatively low reaction

temperatures (200–250°C). Since the reaction is endothermic, a constant heat source is therefore required. The necessary heat can be supplied to the reaction zone via the combustion of methanol and unused hydrogen present in the fuel cell anode exhaust. The overall reaction steam reformation for methanol is given thus:

$$CH_3OH + H_2O \rightarrow CO_2 + 3H_2 \quad \Delta H = +131 \, kJ/mol$$
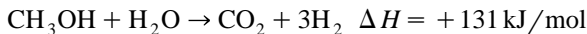
Alternatively, methanol can also be reformed via partial oxidation:

$$CH_3OH + \tfrac{1}{2}O_2 \rightarrow CO_2 + 2H_2 \quad \Delta H = -155 \, kJ/mol$$
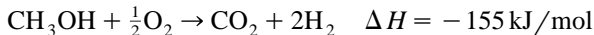
The reaction is exothermic and self-sustaining. Since no heat management sub-system is required, start-up and response characteristics are improved compared to steam reformers. However, it should be noted that the hydrogen yield is lower for respective reactions and is further diluted by the presence of nitrogen from reactant air.

Due to both kinetic and thermodynamic constrains of methanol reforming, significant concentrations of carbon monoxide are produced from both methods of reformation. At typical SPFC operating temperatures ($\leq 85°C$) CO rapidly and strongly adsorbs onto the platinum electrocatalyst surface. Extensive coverage of the platinum surface prevents hydrogen adsorption and electro-oxidation, resulting in a large and rapid decrease in cell performance [11–13]. Although approaches have been made to improve SPFC CO tolerance via either anode air injection or electro-catalyst modification, a stage of CO removal between the reformer and the fuel cells is still currently required [3,13–16]. Methods currently favoured for CO removal include palladium diffusion membranes and selective catalytic oxidation [3,6,17–21]. Whilst the use of diffusion membranes facilitates the supply of ultra-pure hydrogen to the fuel cells, the technology is somewhat compromised by both the high material costs and the operating pressure differential (typically in the region of 20 bars). Alternatively, catalytic CO oxidation may be regarded as a lower cost and more practical method. Appropriate selection of the catalysts should maximise the levels of CO oxidation whilst minimising the extent of hydrogen oxidation, i.e., both high catalyst activity and selectivity.

As partners in the EU funded ''Mercatox'' program [21], Loughborough University has the responsibility of developing a compact catalytic CO oxidation reactor for integration with a methanol steam reformer. In order to meet the program specifications, reactor design has sought to maximise both the compactness and thermal management of the reaction. As such, compact fin heat exchanger technology has formed the basis for the reactor design. The heat exchanger design offers many potential advantages, including compactness, high surface area, all-metal bonding and excellent heat transfer efficiency.

2. Experimental studies

2.1. Test assembly

In order to evaluate the performance of potential oxidation catalysts and reactor designs, a purpose built test facility has been constructed. The test facility, (shown diagrammatically in Fig. 1), consists of a computer controlled gaseous fuel supply system, CO oxidation reactor, temperature control system, vapourised liquid supply system, gas analysis (CO, CO_2 and O_2), and a computerised data acquisition and control system.

The computer controlled fuel supply system employs three gas mass flow controllers each individually controlling the mass flow rate of H_2, CO_2 and CO. Such a system permits fuel compositions typical of that from a reformer
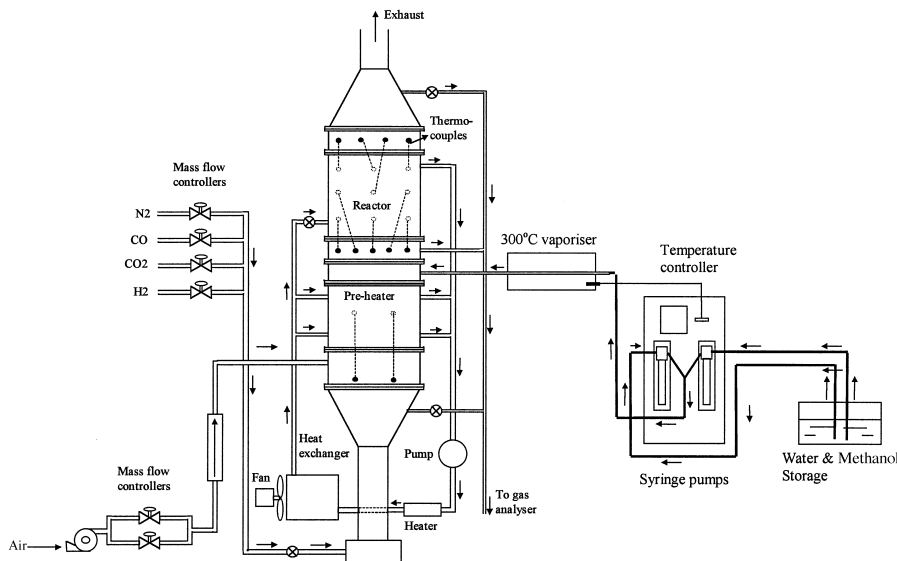

Fig. 1. Schematic of test rig.

to be replicated over a range of flow rates. Water and methanol are pre-mixed and injected via computer controlled syringe pumps. The pumps inject and uptake liquid on consecutive strokes. Through parallel operation of the two pumps continuous injection (and liquid up take) can be achieved. The liquid is introduced into the fuel stream via an electrically heated liquid vaporiser (300°C). The vaporised liquid is then mixed with the pre-heated fuel gas prior to reactor introduction. The temperatures of the fuel pre-heater and CO oxidation reactor are controlled via a programmable temperature controller.

The reactor inlet and exit gas are supplied continuously to CO, CO_2, and O_2 gas analysers. Dynamic measurement of the gas composition is thus allowed. Real-time measurements are recorded using a computerised data acquisition system. The computerised data acquisition system consists of a National Instrument AT-MIO-16 data acquisition card and a Signal Conditioning eXtension for Instruments (SCXI) unit used in conjunction with the data acquisition program (National Instruments LabVIEW software). The status of the gas mass flow controllers and gas analyser outputs are recorded. A total of 16 channels of thermocouples are linked directly to the SCXI data acquisition system and allow both thermal profiling and temperature management of the reactor.

A catalysed reactor used in the studies (complete with attached thermocouple assemblies) is shown in Fig. 2.

The performance of the oxidation reactor was assessed in terms of two primary parameters, namely, catalyst activity and selectivity towards CO in the presence of a large excess of hydrogen. The catalyst activity is defined as the ratio of the reactant consumed divided by its input:

$$A_1 = \frac{\text{Reactant } i \text{ reacted}}{\text{Reactant } i \text{ input}}$$

where i indicates the reactant CO, H_2 or CH_3OH.

In order to reduce system inefficiencies, hydrogen oxidation should be minimised. The catalyst selectivity to-

Table 1
Experimental operating conditions

Catalyst formulation	Pt and Ru/Al_2O_3	
Fuel flow rate (SLPM)	24.33	
GHSV (h^{-1})	2920	
Air flow rate (SLPM)	2.78	
O_2:CO molar ratio equivalent	3:1	
H_2 Inlet content (%)	62.919 (Wet)	67.165 (Dry)
CO_2 Inlet content (%)	20.162 (Wet)	21.689 (Dry Basis)
CO Inlet content (%)	0.498 (Wet)	0.532 (Dry Basis)
CH_3OH Inlet content (%)	0.362 (Wet)	0.390 (Dry Basis)
H_2O Inlet content (%)	6.336 (Wet)	0.000 (Dry Basis)
O_2 Inlet content (%)	2.008 (Wet)	2.143 (Dry Basis)
N_2 Inlet content (%)	7.553 (Wet)	8.063 (Dry Basis)
Methanol (mol min^{-1})	4.696×10^{-3}	
Water (mol min^{-1})	8.218×10^{-2}	

wards CO in the presence of H_2 can be defined as the ratio of the oxygen used for CO oxidation over the total O_2 used for both H_2 and CO oxidation reactions.

$$S_{CO} = \frac{O_2 \text{ used in CO oxidation}}{\text{Total } O_2 \text{ reacted}}$$

Characterisation of the reactor performance (in terms of activity and selectivity) was carried out with respect to:
- Reactor set point temperature,
- O_2 partial pressure effects,
- CO partial pressure effects,
- Fuel flow rates.

Fuel compositions utilised have been based upon actual exit gas analysis data obtained during steady state operation of a methanol steam reformer [22].

Unless otherwise stated, operating conditions and fuel composition data employed in the studies are given in Table 1. Since the reactor gas sample must be dried prior to analysis, inlet gas compositions have also been calculated and presented on a dry gas basis.

3. Results and discussion

Data showing CO, CO_2 and O_2 exit concentrations as a function of reactor operating temperature is presented graphically in Fig. 3. At an operating temperature of approximately 160°C, stable CO exit concentrations of 11 ppm (0.0011%) were obtainable. As the reactor operating temperature was increased to approximately 130°C, the O_2 exit concentration decreased due to the competitive oxidation of CO, H_2, and CH_3OH. At 160°C, the measured O_2 and CO exit concentrations were found to be 0.307% and 11 ppm, respectively. On comparison with the O_2 input concentration of 2.143%, it was found that a total of 1.836% of O_2 has been consumed during the CO oxidation reaction. From the CO oxidation results, since 0.531% (0.532–0.001%) of CO had been oxidised, then this should result in a consumption of 0.265% of O_2. An additional
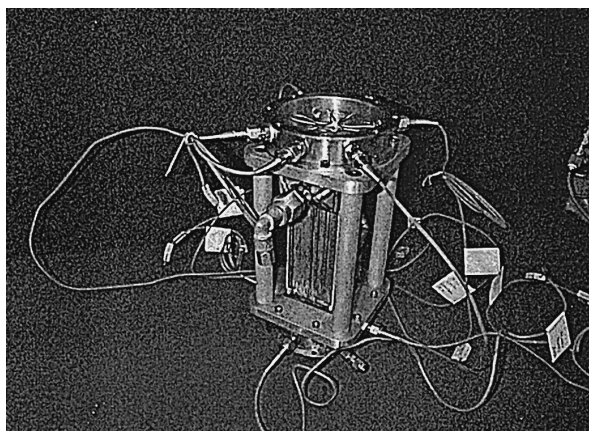

Fig. 2. The 0.5 litre CO oxidation reactor with air injection and thermocouples.
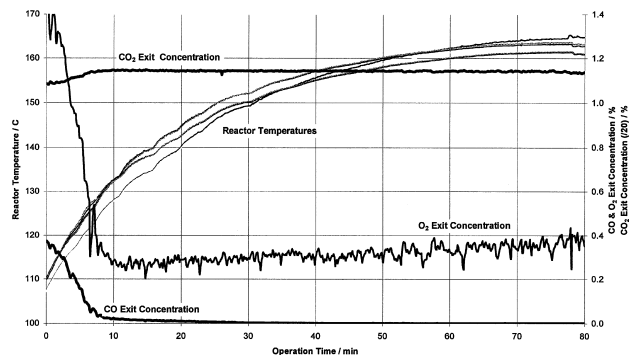
Fig. 3. Reactor CO oxidation w.r.t. reactor operating temperature.

Fig. 4. Reactor activity and selectivity w.r.t. reactor operating temperature.

volumetric concentration of 1.571% of O_2 had therefore reacted with either H_2, CH_3OH or both.

As the reactor temperature was increased over the range 120–145°C, the CO_2 exit concentration increased, indicating the oxidation of CO to CO_2. Upon increasing the reactor temperature above 145°C, the CO_2 exit concentration remains approximately constant since negligible CO remains for oxidation. For a reactor operating temperature of 150°C (and for a CO exit concentration of 11 ppm), the CO_2 exit concentration was measured at 22.87%. When comparing the inlet and exit CO_2 concentrations, it should be noted that since dry gas analysis is performed, H_2O formed via H_2 oxidation is removed prior to analysis. The final CO_2 exit concentration is therefore higher than that generated by CO and methanol oxidation. If the corrected CO_2 input concentration is compared with the exit concentration directly, it can be seen that an increase in the volumetric concentration of CO_2 of approximately 1.18% had occurred. Subtracting the effect of water condensation, this value corresponds to the quantity of CO_2 generated due to CO oxidation (0.531%) and methanol oxidation (0.390%).

The catalyst activity with respect to CO oxidation can be calculated thus:

$$A_{CO} = \frac{0.532\% - 0.0011\%}{0.532\%} = 99.82\%$$

The catalyst selectivity towards CO oxidation was calculated from the measured CO and O_2 input and exit concentrations accordingly:

$$S_{CO} = \frac{0.532\% - 11.7\,ppm}{2(2.143\% - 0.307\%))} = 14.5\%$$

Fig. 4 shows the calculated CO oxidation activity and selectivity as a function of the reactor operating temperature. Catalyst activity was found to increase over the temperature range investigated. For an operating temperature of 150°C, the activity reaches a maximum value of 99.82%. In comparison, the CO oxidation selectivity only increases slightly as reactor temperature increases. For reactor operating temperatures < 125°C, the selectivity remained approximately constant at 14.5%.
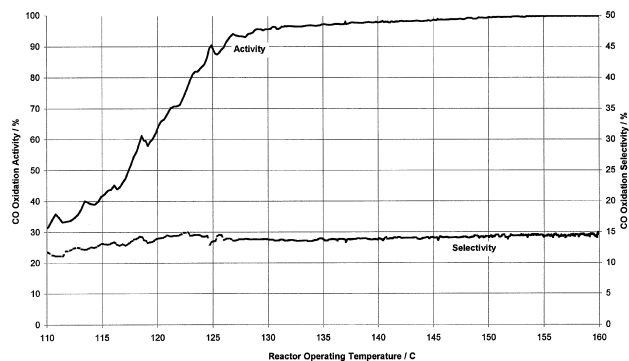
The variation in catalyst activity and selectivity towards CO oxidation as function of temperature may be explained in terms of both the relative rates of CO adsorption and desorption. At lower temperatures, CO coverage on the catalyst surface is extensive. The high chemisorptive bond strength inhibits the dissociative chemisorption of O_2. Steady state kinetics of CO oxidation are therefore limited by the rate of O_2 adsorption and hence, both the CO oxidation selectivity and activity are low. Upon increasing the temperature, the rate of CO desorption increases, and thus the number of catalyst sites for O_2 adsorption is increased. CO oxidation activity, therefore, increases. However, at such elevated temperatures, the kinetics of H_2 chemisorption will also be increased, resulting in increased H_2 oxidation and reduced catalyst selectivity towards CO oxidation. Hence, CO oxidation selectivity is not increased significantly at higher reaction temperatures.

Fig. 5 shows the reactor activity for operation with increasing fuel flow rates. It can be seen that for fuel flows of up to 150 SLPM, a single 0.5 litre reactor is capable of reducing the inlet CO concentration by at least 85%. The inlet gas composition was as detailed in Table 1, i.e., an air flow equivalent to $3O_2$:CO was maintained throughout. The reactor set point temperature was 160°C.

For fuel flow rates ≥ 100 SLPM, and in order to achieve fuel CO output concentrations of < 20 ppm it was
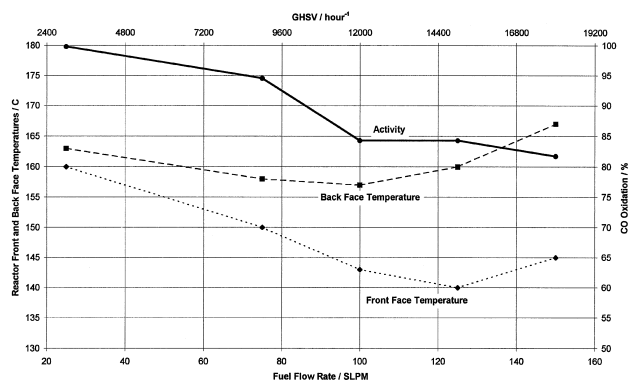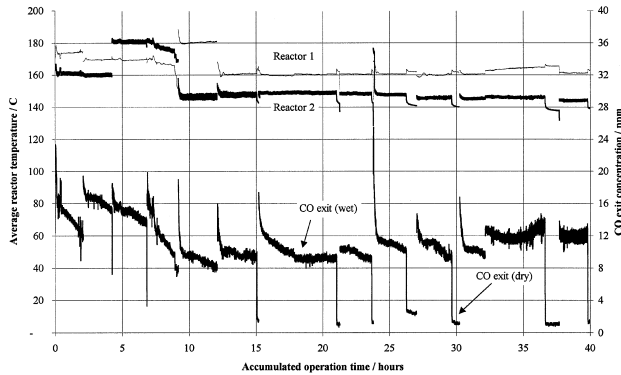

Fig. 5. Fuel flow rate effects upon reactor activity.

Fig. 6. Steady state CO exit concentration of the two-stage reactor.

Fig. 8. Two-stage reactor performance w.r.t. CO input concentration.

found to be necessary to increase the total reactor volume to 1 litre. This was achieved by the incorporation of a second 0.5 litre precious metal washcoated heat exchanger into the test assembly. The reactors were operated in a series configuration and each with individual air supply. Typical performance of the 1 litre reactor under optimised steady state conditions can be seen in Fig. 6. At a fuel flow rate typically equivalent to SPFC power output of 5 kW, acceptable CO output concentrations of 10–20 ppm were obtained. In addition, when the reactor was operated under dry fuel conditions then CO outputs of < 5 ppm were achieved.

The reactor performance was assessed for a range of CO input concentrations, i.e., 500–10,000 ppm (69.6% H_2, 7.0% H_2O, 0.4% CH_3OH and balance CO_2). The fuel flow rate was maintained at 100 SLPM and the air flow rate was adjusted with the CO inlet concentration such that a molar equivalent of $4O_2$:CO was maintained. The reactor temperature was controlled at 160°C for all CO input concentrations. Results showing CO output concentrations and the calculated catalytic activity and selectivity are presented in Fig. 7.

For fuel flow rates > 100 SLPM and for varying CO input concentrations it was again necessary to employ a dual stage reactor configuration, such that the CO concentration could be reduced to acceptable levels for SPFC
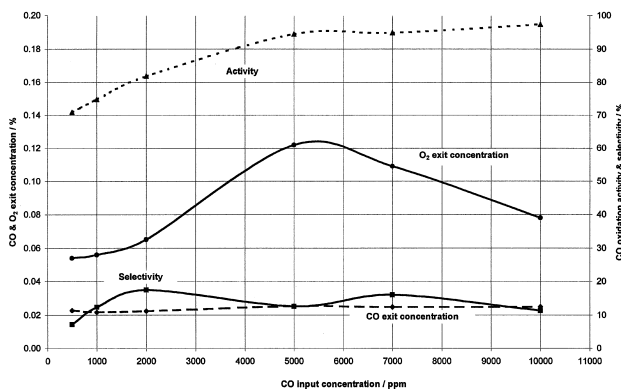
utilisation. Fig. 8 shows the measured CO output for the dual stage reactor (2×0.5 l) as a function of inlet CO concentration, i.e., 1000–7000 ppm (69.6% H_2, 7.0% H_2O, 0.4% CH_3OH and balance CO_2) and air flow rate to each reactor. A fuel flow rate of 150 SLPM was used in all tests. The reactors were controlled within the temperature range 150–160°C.

From the results presented in Fig. 8, it can be seen that CO output concentrations of ≤ 10 ppm were achieved for a range of CO inputs. The operation of the dual stage reactor was therefore successful in reducing CO concentrations to acceptable levels for SPFC utilisation (i.e., ≤ 10 ppm) for a range of typical steam reformer output compositions containing up to 0.7% CO.

The calculated catalyst activity and selectivity towards CO oxidation under varying O_2 input concentrations are shown in Fig. 9. A reactor set point temperature of 160°C and fuel flow rate of 25 SLPM were used. (Fuel compositions were as detailed in Table 1.) As expected, it was found that the catalyst CO oxidation activity and selectivity were proportional and inversely proportional, respectively to the O_2 concentration injected into the reactor. The relationship between O_2 inlet partial pressure and catalyst selectivity and activity towards CO oxidation may be explained in terms of the extent of dissociatively adsorbed O_2 upon the catalyst surface. At lower O_2 partial pressures and at a reactor temperature of 160°C, the catalyst surface is extensively covered with CO. The rate of O_2 reaction

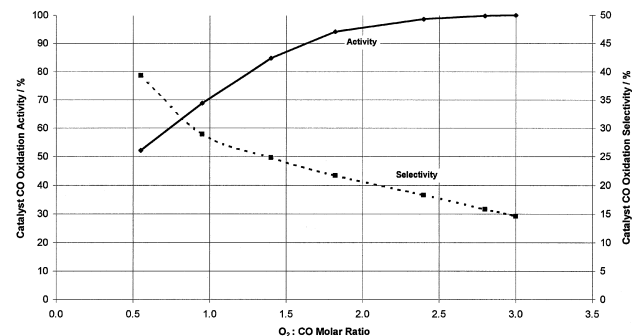Fig. 7. Single stage reactor performance w.r.t. CO input concentration.

Fig. 9. Effect of oxygen pressure upon catalyst activity and selectivity.

Table 2
Mass and energy conservation equations

Hydrogen flow rate		$\dot{M}_{fuel} = \dfrac{I}{Fz\eta_{H_2}n_{H_2}}$
CO oxidation	Reaction	$CO + 1/2O_2 \rightarrow CO_2$
		$\Delta H_{CO,reaction} = -283.0\,kJ/mol$
		$H_2 + 1/2O_2 \rightarrow H_2O$
		$\Delta H_{H_2,reaction} = -285.8\,kJ/mol$
		$CH_3OH + 3/2O_2 \rightarrow CO_2 + 2H_2O$
		$\Delta H_{CH_3OH,reaction} = -276.1\,kJ/mol$
	Energy calculation	Energy input　　$\dot{E}_{reformate\ and\ air} = \sum_{n=1}^{7}\dot{M}_n c_{p,n}(T_o - T_{reformate\ or\ ambient})$
		Energy of reaction　　$[CO]_{reacted} = A_{CO}[CO]_{in}$
		$[H_2]_{reacted} = \{[O_2]_{in} - [O_2]_{out} - [O_2]_{CO} - [O_2]CH_3OH\}/2$
		$[CH_3OH]_{reacted} = A_{CH_3OH}[CH_3OH]_{in}$
		$\dot{E}_{reaction} = \sum_{k=1}^{3}\Delta H_{k,reaction}[k]_{reacted}$
		Energy outlet　　$\dot{E}_{outlet} = \sum_{j=1}^{7}\dot{m}_j c_{p,j}(T_o - T_{outlet})$
		Energy conservation　　$\dot{E}_{outlet} = \dot{E}_{reformate\ and\ air} + \dot{E}_{reaction}$

with CO and hence catalyst activity is lower. At increased O_2 partial pressures, O_2 adsorption is increased which results in increased rate of reaction with adsorbed CO. However upon further increasing the O_2 partial pressure, not only is more adsorbed O_2 available for reaction but also due to the high rate of CO oxidation, a greater number of catalytic sites will also become available for additional H_2 oxidation. A decrease in the calculated catalyst selectivity results.

4. Theoretical study

In order to simulate the chemical reaction and thermal management of the reactor, a simplified theoretical model has been developed based on mass and energy conservation. Catalyst activity and selectivity calculations based upon experimental data have also been introduced into the model. The model (Table 2) consists essentially of two major parts:

· Simulated rate of CO oxidation.
· Required SPFC H_2 flow rate.

Three oxidation reactions are considered in the simulation, i.e., carbon monoxide, hydrogen and methanol. It is possible that a small amount of methanation may also

occur in the reactor. However, the rate of this reaction has been assumed to be negligible for the reactor operating temperatures utilised and has not been included in the calculation. The fuel flow rate required by SPFC stacks is linearly proportional to the stack's electrical current output. A fuel flow rate of 25 SLPM and composition of 69.6% H_2, 22.4% CO_2, 0.6% CO, 0.4% CH_3OH and 7.0% H_2O was used in all calculations. The reactor set-point temperature was 160°C.

Fig. 10 shows the measured and calculated CO exit concentration for the reactor for increasing O_2:CO molar ratios. It can be seen that the CO exit concentration decreases as the O_2:CO molar ratio increases. This is due to both the increased O_2 partial pressure increasing the rate of CO oxidation and the increased air injected into the CO reactor diluting the gaseous fuel supply. The dilution effect results in a 2.7%–7.8% decrease in the volumetric concentration of CO when the O_2:CO molar ratio is increased from 1:1 to 3:1. The small difference between the measured and calculated data is due to the inclusion of H_2O content in the fuel mixture calculations, whereas H_2O is removed during experimental exit gas analysis.

Fig. 11 shows the calculated exit concentrations of H_2. Due to injected air dilution, the volumetric concentration of H_2 decreases as the O_2:CO molar ratio increases.
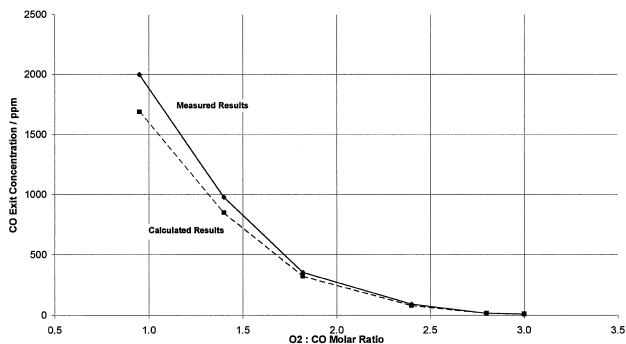

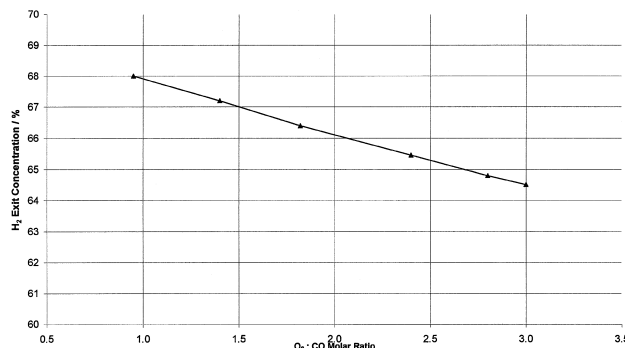Fig. 10. Comparison of measured and calculated CO exit concentration.

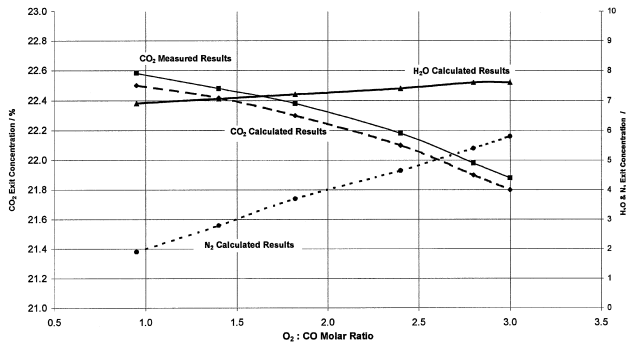Fig. 11. Calculated H_2 exit concentration.

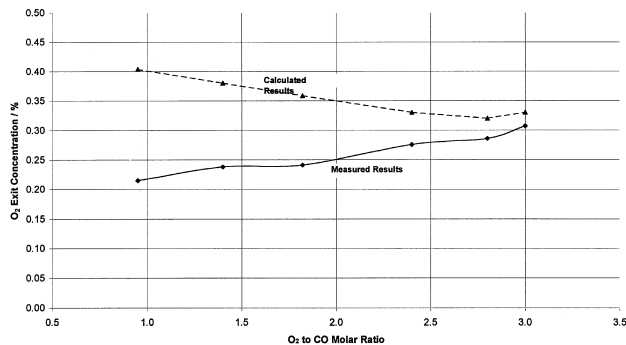Fig. 12. Comparison of measured and calculated CO_2, N_2, and H_2O exit concentrations.

Fig. 13. Comparison of measured and calculated O_2 exit concentration.

Fig. 12 shows the measured and calculated CO_2, H_2O, and N_2 exit concentrations with increasing O_2:CO molar ratios. It can be seen that the CO_2 exit concentration decreases as O_2:CO molar ratio increases due to air dilution. As the quantity of air injected into the reactor is increased more O_2 is available for H_2 oxidation and thus both H_2O and N_2 concentrations in the reactor exit stream increase.

Fig. 13 shows the measured and calculated O_2 exit concentrations. Unlike the calculated exit concentrations of CO and CO_2, the calculated O_2 concentration does not show such good agreement with the measured results. The calculated O_2 exit concentration decreases slightly as O_2:CO molar ratio increases, while the measured O_2 exit concentration was found to increase. This disparity in the results may be due to the assumption that all methanol is oxidised under the test conditions employed. In practice, this may not be correct, with decreased methanol oxidation occurring at lower O_2 partial pressures.

5. Conclusions

(i) A simplified CO oxidation reactor simulation model has been developed. By calculating the catalyst CO oxidation activity and selectivity from experimental data, the model can simulate the exit fuel compositions from the reactor. Comparison of the calculated and experimental results shows good agreement in terms of measured CO, O_2 and CO_2 concentrations. The model allows the H_2 content in the fuel stream presented to the fuel cell to be calculated. Calculations have also established the basis for further research regarding improving catalyst CO oxidation activity and selectivity.

(ii) A critical issue for successful reactor operation in terms of reducing CO concentrations to levels acceptable for SPFC use, is that of thermal management. A compact fin aluminium heat exchanger has been identified as being suitable for catalyst washcoating due to its high surface area and excellent heat transfer efficiency. An experimental test rig utilising such compact fin aluminium heat exchanger technology has been constructed and evaluated at Loughborough University.

(iii) Through the utilisation of proprietary precious metal based catalyst technology a dual stage reactor has been developed by the Fuel Cell Group at Loughborough University. The technology has allowed CO concentrations to be reduced from 7000 to ≤ 11 ppm at flow rates up to 150 SLPM and with fuel compositions typically produced by methanol steam reformation. The reactor volume used was 1 l.

(iv) Both CO oxidation activity and selectivity were calculated and analysed. It was found that the reactor operating temperature affects both catalyst performance parameters. At an operation temperature of 160°C, the CO oxidation activity was calculated to be 99.8% with the CO selectivity calculated to be 21.2%.

(v) The catalyst CO oxidation activity and selectivity was also found to be affected by O_2 partial pressure. The CO oxidation activity increases as O_2:CO molar ratio increases. At a molar ratio of 3:1, the activity was calculated to be 99.8%. However, the CO oxidation selectivity decreased as O_2:CO molar ratio was increased. At a molar ratio of 3:1, the selectivity was calculated to be 21.2%.

References

[1] S.G. Chalk et al., J. Power Sources 71 (1/2) (1998) 26.
[2] F. Panik, J. Power Sources 71 (1/2) (1998) 36.
[3] S. Kawatsu, J. Power Sources 71 (1/2) (1998) 150.

[4] M.A.B. Nurdin, Proc. Commercializing Fuel Cell Vehicles, Frankfurt, Oct. 1997.

[5] G.A. Hards, T.R. Ralph, Platinum Met. Rev. 39 (1) (1995) 9.

[6] N. Edwards et al., J. Power Sources 71 (1/2) (1998) 123.

[7] S. Golunski, Platinum Met. Rev. 42 (1) (1998) 2.

[8] G. Hornburg, Proc. Commercializing Fuel Cell Vehicles, Frankfurt, Oct. 1997.

[9] W.P. Teagen et al., J. Power Sources 71 (1/2) (1998) 80.

[10] W.L. Mitchell et al., SAE Paper 952761, 1995.

[11] C.M. Seymour, J. Power Sources 37 (1992) 155.

[12] R.A. Lemons, J. Power Sources 29 (1990) 251.

[13] S. Gottesfeld, S. Pafford, J. Electrochem. Soc. 135 (1988) 2651.

[14] U.S. Patent 4,910,099.

[15] G.A Hards et al., Proc. Fuel Cell Seminar, Orlando FL, Nov. 1996, p. 544.

[16] S. Kawatsu et al., Proc. Fuel Cell Seminar, Orlando FL, Nov. 1996, p. 262.

[17] B. Emonts et al., J. Power Sources 71 (1/2) (1998) 288.

[18] S.E. Golunski, J.G. Reinkingh, ETSU Report F/02/00137.

[19] S.E. Golunski, A.N.J. Van Keulen, J.G. Reinkingh, ETSU Report F/02/00118.

[20] P.L. Adcock, C.D. Dudfield et al., Proc 29th Int. Symp. Auto. Tech. and Automation, Florence, June 1996, p. 287.

[21] C.D. Dudfield, P.L. Adcock, R. Chen, Proc. Fuel Cell Seminar, Palm Springs, CA, Nov. 1998, p. 341.

[22] R.K.A.M. Mallant (Ed.), 2nd Periodic Report, E.U. Contract No JOU-CT92-0143.